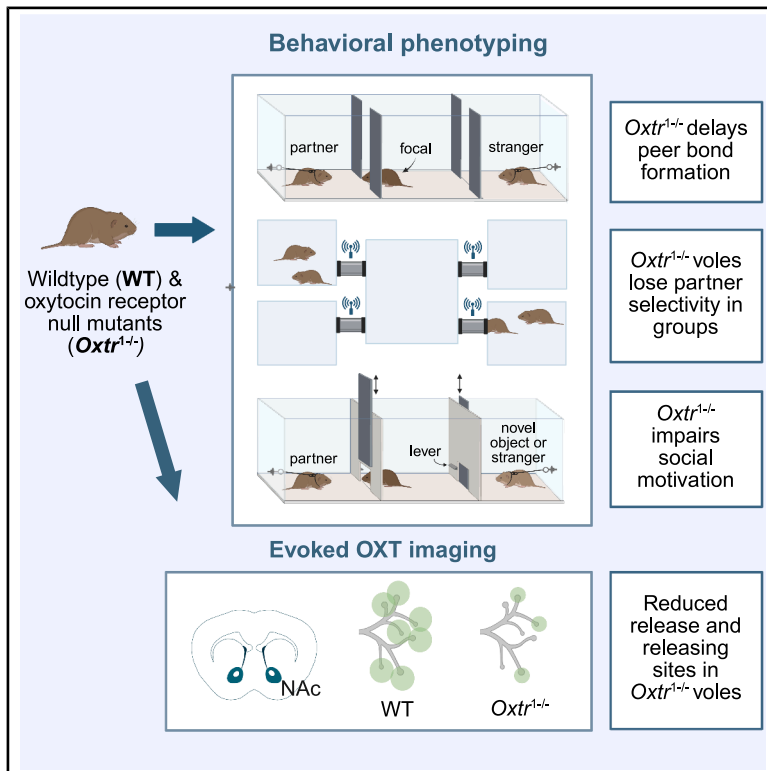


Oxytocin receptors mediate social selectivity in prairie vole peer relationships

Graphical abstract



Authors

Alexis M. Black, Natsumi Komatsu, Jiaxuan Zhao, ..., Devanand S. Manoli, Markita P. Landry, Annaliese K. Beery

Correspondence

landry@berkeley.edu (M.P.L.),
abeery@berkeley.edu (A.K.B.)

In brief

Black & Komatsu et al. examine the role of oxytocin receptor signaling in selective peer relationships, finding that female $Oxtr^{1-/-}$ prairie voles exhibit delayed bond formation, unstable relationships, reduced partner reward, and lower nucleus accumbens oxytocin release. These findings demonstrate a critical role for oxytocin receptors in peer relationship selectivity.

Highlights

- Female $Oxtr^{1-/-}$ prairie voles are slow to form new selective peer relationships
- Females lacking OXTR have reduced partner-specific and general social motivation
- Females lacking OXTR exhibit less stranger avoidance and aggression
- Development without OXTR reduces nucleus accumbens oxytocin release

Article

Oxytocin receptors mediate social selectivity in prairie vole peer relationships

Alexis M. Black,^{1,6} Natsumi Komatsu,^{2,6} Jiaxuan Zhao,³ Scarlet R. Taskey,¹ Nicole S. Serrano,¹ Ruchira Sharma,⁴ Devanand S. Manoli,⁴ Markita P. Landry,^{2,5,*} and Annaliese K. Beery^{1,5,7,*}

¹Department of Integrative Biology, University of California, Berkeley, Berkeley, CA 94720, USA

²Department of Chemical and Biomolecular Engineering, University of California, Berkeley, Berkeley, CA 94720, USA

³Department of Molecular and Cellular Biology, University of California, Berkeley, Berkeley, CA 94720, USA

⁴Department of Psychiatry and Behavioral Sciences, University of California, San Francisco, San Francisco, CA 94158, USA

⁵Department of Neuroscience, University of California, Berkeley, Berkeley, CA 94720, USA

⁶These authors contributed equally

⁷Lead contact

*Correspondence: landry@berkeley.edu (M.P.L.), abeery@berkeley.edu (A.K.B.)

<https://doi.org/10.1016/j.cub.2025.07.042>

SUMMARY

Friendships, or *selective peer relationships*, are a vital component of healthy social functioning in humans, and deficits in these relationships are associated with negative physical and mental health consequences. Like humans, prairie voles are among the few mammalian species that form selective social bonds with both peers and mates, making them an excellent model for the mechanistic investigation of selective social attachment. Here, we explored the role of oxytocin receptors in selective peer attachment using female prairie voles lacking a functional oxytocin receptor gene (*Oxtr*^{1-/-}). We found that *Oxtr*^{1-/-} animals exhibited significant delays in peer relationship formation compared with wild-type animals. Oxytocin receptor function also contributed to the maintenance of peer bonds, as *Oxtr*^{1-/-} voles displayed reduced relationship stability and lost selective attachments rapidly in a multi-chamber, group-living habitat. *Oxtr*^{1-/-} voles also showed deficits in general social reward as well as selective social reward for a peer partner over an unfamiliar conspecific. Evoked oxytocin release in the nucleus accumbens was reduced in male and female *Oxtr*^{1-/-} animals compared with their wild-type counterparts, indicating that these voles do not have a compensatory increase in oxytocinergic signaling. Together, these data indicate that oxytocin receptors influence the formation, persistence, and reward value of peer relationships.

INTRODUCTION

Strong and supportive social relationships are crucial for mental well-being, stress resilience, and longevity in social animals,^{1–5} while difficulty forming or maintaining relationships is a hallmark of numerous neuropsychiatric disorders.^{6,7} Humans form myriad social attachments across a lifespan, including relationships with parents, offspring, romantic partners, group members, and friends. A common feature of these close relationships is *selectivity*, or the preference to spend time with specific social partners over novel individuals. Friendships, referred to here as selective peer relationships, are functionally distinct from reproductive mate relationships and also integral for social health and well-being.^{5,8–10} Nevertheless, we lack an understanding of the neural mechanisms that support selective peer relationships.

Across the animal kingdom, the neuropeptide oxytocin has been implicated in various social processes, from social recognition and reward to mate bond formation.^{11–14} The repeated convergence of complex social behaviors on evolutionarily conserved neural circuits—such as those involving oxytocin signaling—underscores the value of investigating shared neural

pathways across diverse taxa as well as unique mechanisms underlying species-specific specializations in social behavior. Growing evidence suggests that oxytocin signaling and receptor distribution play important roles in mediating social interactions between same-sex peers,^{15–17} but the role of oxytocin signaling in mediating and reinforcing the development of *selective* social bonds in peer relationships remains limited.^{18–20}

Prairie voles have become an essential model organism for understanding the basis of complex social relationships, including social monogamy and selective affiliation.^{21–23} Unlike most traditional laboratory rodents,^{24,25} but similar to humans, prairie voles form selective social bonds with both mates and peers, displaying a robust preference to interact with familiar “partners” over novel “strangers.”^{26,27} Foundational pharmacological studies investigating the role of oxytocin signaling in prairie vole mate relationships show that the central and region-specific blockade of oxytocin receptors (OXTRs) impair mate bond formation,^{28,29} while intracranial infusion of oxytocin accelerates the onset of partner preference.^{29–31} In particular, these studies have highlighted the nucleus accumbens (NAc) as a critical region for mediating oxytocin-dependent effects on social attachment.^{32,33} These pharmacological findings

provide seminal insights into understanding the role of oxytocin signaling in relationship formation; however, early work examined only *mate* attachments.

The novel development of transgenic prairie voles lacking functional OXTRs has paved the way for longitudinal studies of the oxytocin system in social bond formation and other complex social behaviors. Recent studies of OXTR null mutant (*Oxtr*^{1-/-}) voles found that functional OXTRs are not required for partner preference formation between mates after 1 week of cohabitation,³⁴ but mate relationship formation in *Oxtr*^{1-/-} animals was impaired after *shorter* cohousing intervals that are normally sufficient for bond formation (6 h for females and 5 days for males).³⁵ These results reinforce early findings from pharmacological approaches, indicating that oxytocin signaling mediates *early* social interactions, accelerates bond formation, and supports the rejection of strangers in reproductive relationships. The concept that oxytocin activity facilitates efficient mate relationship formation parallels existing theories regarding the role of oxytocin in social salience and the amplification of relevant social information.³⁶⁻³⁸ Such studies expand our understanding of the role of OXTRs in mate bond formation throughout extended periods of cohabitation, but *peer* social relationships remain less well understood.

In the present study, we used female *Oxtr*^{1-/-} prairie voles to examine the role of OXTRs in selective peer social relationships. Wild-type (WT) female prairie voles rapidly form selective social bonds with new peers in adulthood and work harder to access familiar versus unfamiliar peers.^{20,26,39-41} Across multiple behavioral testing paradigms, we found that OXTRs are necessary for early-stage peer bond formation, lasting peer attachment, and selective social reward—specifically in peer contexts. Furthermore, to assess how genetic disruption of OXTR affects oxytocin signaling, we employed recently developed synthetic optical probes that enable real-time imaging of extracellular oxytocin dynamics with high spatial and temporal resolution in acute brain slices. Real-time oxytocin imaging revealed that both male and female *Oxtr*^{1-/-} animals have reduced evoked oxytocin release in the nucleus accumbens.

RESULTS

Bond formation with a peer partner is delayed in *Oxtr*^{1-/-} females

We explored how OXTRs impact peer relationship formation by assessing the timeline of peer bond formation in *Oxtr*^{1-/-} and WT (*Oxtr*^{+/+}) females using partner preference tests (PPT, Figure 1A). WT and *Oxtr*^{1-/-} focal females were pair-housed with a same-sex partner from weaning and tested in adulthood (PPT A: lifetime partner). Next, focal voles were paired with a new, unrelated WT peer partner, and two additional PPTs were carried out 24 h (PPT B) and 7 days (PPT C) into cohabitation to assess new bond formation. We quantified the duration spent in side-by-side contact (huddling) with the partner and the stranger across the 3-h test to characterize social preference. *Oxtr*^{1-/-} females displayed fewer bouts of aggression toward strangers across all three PPTs compared with WT animals (Figure 1B). *Oxtr*^{1-/-} females formed peer bonds with the lifetime and 7-day “long-term” partners (Figures 2C and 2E) but exhibited significant deficits in the early stages of relationship formation (Figure 2D). There were no significant differences in

time spent alone in the center chamber across the three tests, or in physiological characteristics such as internal body temperature or adult body weight (Table S1).

Oxtr^{1-/-} females are more gregarious and display less stable peer relationships compared with WT females in free-moving groups

We measured the strength and stability of peer bonds within newly formed groups of freely behaving WT and *Oxtr*^{1-/-} females by examining how social patterns changed as pairs became part of larger groups in a semi-naturalistic habitat over 6 days of cohabitation. Each group included two pairs of previously established peer partners (4 voles in total), all of the same genotype. Voles were implanted with RFID tags and placed into a multi-chambered habitat equipped with 8 RFID antennas (Figure 2A) to collect and analyze positional data without human disturbance.^{42,43}

OXTR function had a major impact on social selectivity. In the first 3 h of cohabitation (the duration of a PPT), and across the first day, *Oxtr*^{1-/-} voles spent a smaller proportion of their total social time with their initial partner, suggesting lower partner selectivity compared with WT voles (Figures 2B and 2C). *Oxtr*^{1-/-} voles were not only less selective than WT voles but also cohoused with their partner for a duration just below that expected by chance, indicating a complete lack of partner specificity (Figure 2C). By the end of the cohousing period (day 6), there was no difference in partner selectivity between genotype groups, with both groups averaging about half of their total social time with their initial partner (Figure 2D). This convergence in partner selectivity between genotype groups was concurrent with increased time spent in larger groups (i.e., with all voles in the habitat) throughout the week, as shown in Figure 2E. Both genotype groups spent similar amounts of time in groups, but *Oxtr*^{1-/-} voles formed smaller groups, on average, compared with WT voles (Figure 2E). Both genotype groups huddled more with new group members after the week of cohousing compared with the pre-test condition, indicating that social relationships developed within each group of voles throughout group living (Figure S1A).

Oxtr^{1-/-} females display deficits in social reward

We quantified selective social motivation in WT and *Oxtr*^{1-/-} females using an operant lever-pressing task coupled with a social choice (Figure 3A). We tested animals in three contexts with various target rewards: (1) peer partner versus stranger, (2) mate partner versus stranger, and (3) mate partner versus non-social reward (novel object). We analyzed the number of rewards of each type (achieved via 4 presses at the respective target lever) across 3 days of testing as a metric of social motivation.

WT females in peer partnerships were more motivated to access their partner than a stranger, whereas *Oxtr*^{1-/-} females exhibited no selectivity in peer social reward (Figure 3B). Both WT and *Oxtr*^{1-/-} were more motivated to access a mate partner versus a stranger (Figure 3C). However, only WT animals were more motivated to access their mate partner versus a non-social reward. Additionally, *Oxtr*^{1-/-} females showed greater motivation to access this non-social stimulus compared with WT females (Figure 3D). Further behavioral metrics are depicted in Figures S3A–S3C. We found no difference between genotype groups in the extinction of pressing behavior (Figure S3D).

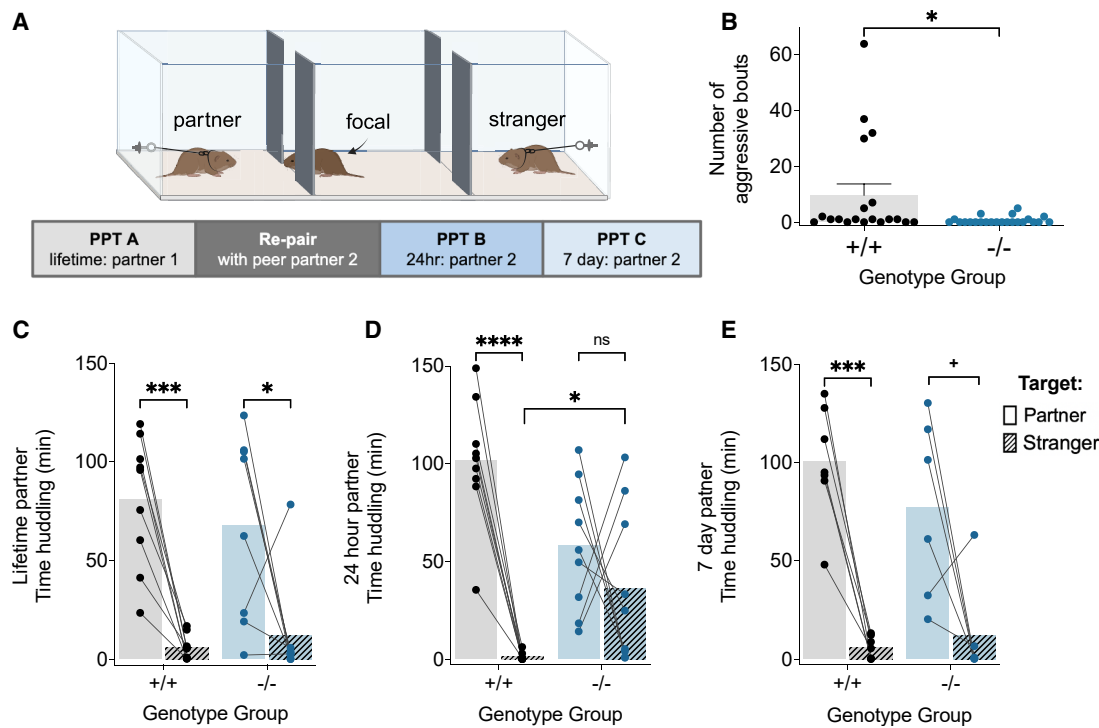


Figure 1. *Oxtr*^{1-/-} females exhibit reduced aggression and delayed peer partner preference formation

(A) Partner preference test (PPT) apparatus and testing timeline. Apparatus figures created with BioRender.

(B) Across PPTs, WT (+/+) females were more aggressive than OXTR null mutants (-/-).

(C) Both WT and *Oxtr*^{1-/-} females showed a significant preference to huddle with their lifetime (4+ week) partner versus a stranger.

(D) After 24 h of cohabitation with the new peer partner, huddling duration was influenced by the interaction of genotype and social target (partner/stranger). WT females showed huddling preference for a 24-h peer partner, whereas *Oxtr*^{1-/-} voles did not. *Oxtr*^{1-/-} voles also spent more time huddling with the same-sex stranger compared with the WT group.

(E) Both WT and *Oxtr*^{1-/-} females showed a preference for their peer partner after a week of cohabitation.

See statistics (model results and pairwise comparisons) reported in Table S1.

+ denotes $p = 0.0527$, * $p < 0.05$, ** $p < 0.01$, *** $p < 0.001$, and **** $p < 0.0001$.

Error bars denote standard error of the mean.

Oxytocin signaling in the nucleus accumbens is reduced in *Oxtr*^{1-/-} voles

Given that early bond formation, partner selectivity, and social reward were impaired in *Oxtr*^{1-/-} females, we examined whether oxytocin signaling is enhanced or downregulated in the absence of functional OXTR. We analyzed *ex vivo* oxytocin release kinetics in WT and *Oxtr*^{1-/-} voles of both sexes following behavioral testing, using recently developed synthetic oxytocin nanosensors “nanOx.”⁴⁴ nanOx is based on single-walled carbon nanotubes noncovalently functionalized with a single-stranded DNA sequence that selectively modulates fluorescence intensity upon interaction with oxytocin (Figure S3A) but not with vasopressin. This synthetic approach provides versatility across species as it does not require genetic manipulation,^{45,46} and it allows for real-time imaging of extracellular oxytocin with high spatiotemporal resolution.^{44,47} We imaged electrically evoked oxytocin release in the nucleus accumbens (Figures 4A–4C), a region in which OXTR expression and oxytocin signaling have been strongly implicated in pair bonding with mates in prairie voles.^{28,32,33}

We quantified several features of oxytocin signaling dynamics (Figures S3B–S3I). First, we quantified the number of oxytocin

release sites by calculating the regions of interest within the field of view that showed statistically significant increases in nanOx fluorescence upon stimulation. We also quantified oxytocin release by calculating the nanOx fluorescence change ($\Delta F/F_0$) of the full imaging field of view (integrated $\Delta F/F_0$) and also of each release site ($\Delta F/F_0$ across active release sites). Lastly, we quantified the time needed for oxytocin clearance from each release site. *Oxtr*^{1-/-} voles had reduced oxytocin release in the overall imaging field of view (integrated $\Delta F/F_0$) relative to their WT counterparts (Figure 4E). On a subcellular level, *Oxtr*^{1-/-} voles showed fewer oxytocin release sites (Figure 4F), with each release site also exhibiting diminished oxytocin release relative to oxytocin released from WT release sites (Figure 4G). These data suggest a reduction in the number of oxytocin release sites and amount of oxytocin release per site and across sites in the absence of OXTR. We found no statistically significant difference in the oxytocin clearance rates across genotype (Figure 4H). Motivated by recent studies revealing oxytocin-induced modulation of dopamine pathways in mice and rats,^{48–52} we also assessed whether *Oxtr*^{1-/-} mutation impacted accumbal dopamine release in prairie voles using a near-infrared catecholamine nanosensor (nIRCcat).⁴⁷ We found that *Oxtr*^{1-/-} voles exhibited significantly

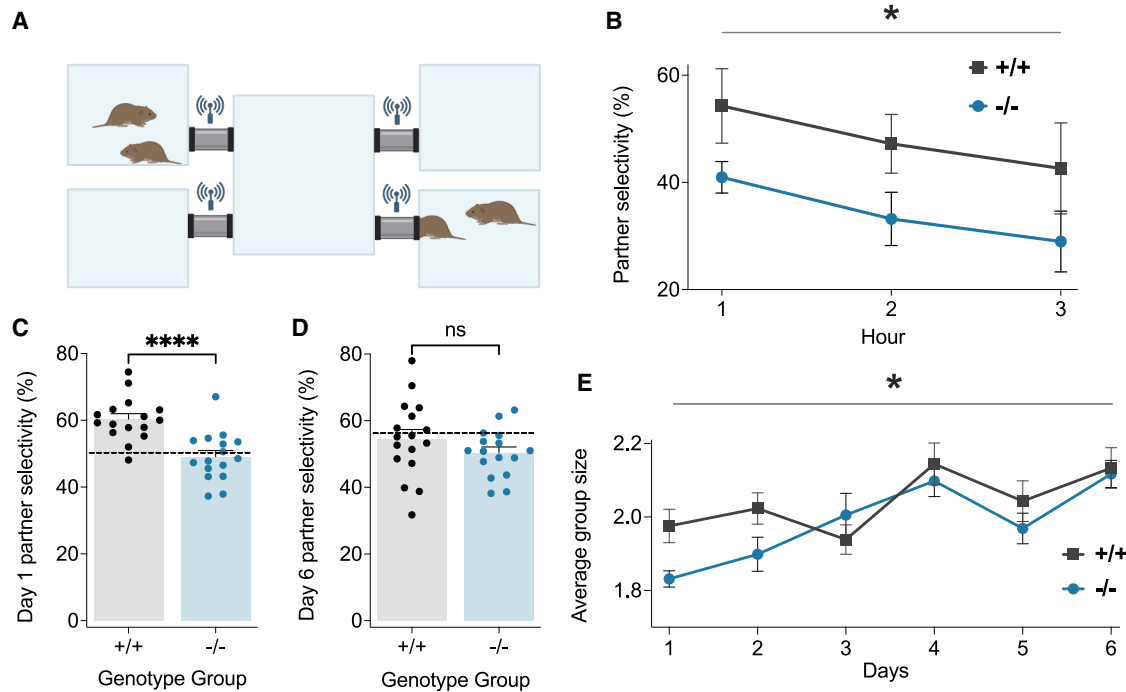


Figure 2. *Oxtr*^{-/-} females lose track of established relationships and integrate with novel peers in group habitats more quickly than WT females

(A) Five-chamber habitat with RFID ring antennas at each end of the connecting tubes.

(B) *Oxtr*^{-/-} voles showed a lower magnitude of partner selectivity (% partner selectivity = [time with established partner/total time social] × 100) across the first 3 h of group living. “Genotype” and “test day” also interacted significantly to affect partner selectivity across the week (see Table S2).

(C) On day 1 of group cohabitation, *Oxtr*^{-/-} females spent a lower percentage of their total social time with their partner compared with WT females. The dashed line (51%) indicates the partner selectivity expected by chance on day 1, given cohabitation in the group sizes exhibited on that day (see STAR Methods). WT females were significantly more partner selective than expected by chance, whereas *Oxtr*^{-/-} exhibited no partner selectivity.

(D) By day 6, there was no difference in partner cohabitation by genotype. The dashed line (56%) indicates the partner selectivity expected by chance given cohabitation in the group sizes exhibited on that day, and neither group exhibited selective bias toward cohabiting with their original partner.

See also Figures S1B and S1C.

(E) On day 1 and across the week, *Oxtr*^{-/-} animals cohabited in smaller groups compared with WT animals.

See statistics reported in Table S2. Error bars denote the standard error of the mean. * *p* < 0.05, **** *p* < 0.0001.

slower dopamine clearance relative to their WT counterparts (Figure S4).

DISCUSSION

We find that the loss of OXTR disrupts selective peer attachment, impacting the formation, stability, and reward value of peer social relationships.

OXTRs modulate the speed of peer bond formation

Both WT and *Oxtr*^{-/-} voles showed peer partner preference after extended (week-long and lifetime) cohabitation with a peer partner. In contrast, *Oxtr*^{-/-} females did not form partner preferences after 24 h of cohabitation—a duration that is sufficient to induce robust partner preferences in unmanipulated WT animals.^{26,31,53} Abolishing OXTR signaling in female prairie voles thus delayed the formation of selective social relationships with peers at 24 h, while longer-term social bonding remained unaffected. These results reinforce prior pharmacological findings by indicating that oxytocin signaling mediates early social interactions and timely bond formation.^{28,29,32,54–56} Delays in peer relationship formation parallel deficits found in mate bond formation in *Oxtr*^{-/-}

animals.³⁵ Together, these data provide further evidence that oxytocin signaling plays a role in the formation of new selective relationships and acts to amplify relevant social information to efficiently encode salient social contexts.^{37,38} Although OXTRs play a crucial role in efficient bond formation, the eventual development of a selective attachment must be facilitated by other mechanisms.

OXTRs are necessary for selectivity in peer groups

Beyond examining the role of OXTRs in dyadic interactions, we probed their role in selective peer social behavior within groups. Unlike monogamous pair bonds with mates, peer relationships in prairie voles are not exclusive and are formed between multiple members of a group.⁵⁷ In contrast to WT animals, we found that *Oxtr*^{-/-} voles immediately “lost track” of their original partner during free interaction. Indeed, even in the first 24 h of cohousing, *Oxtr*^{-/-} voles spent no more time with their initial partner than would be expected by chance, indicating a lack of selectivity and an increase in gregarious social behavior. These results suggest that even when *Oxtr*^{-/-} voles display peer partner preference, the selectivity of their relationships is less stable in broader and more ecologically relevant social settings. It is possible that

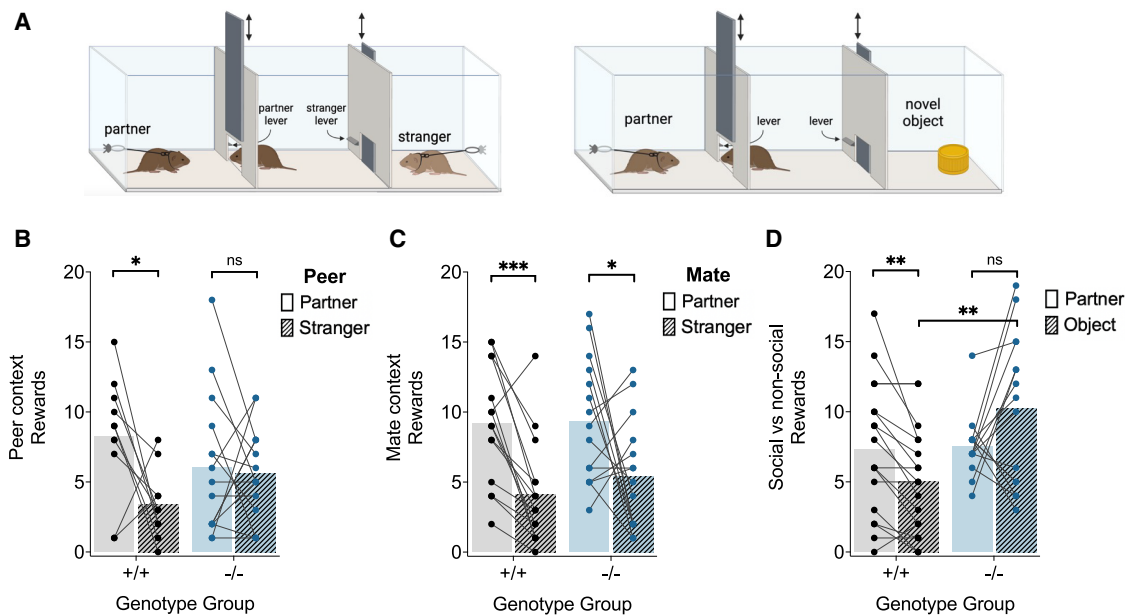


Figure 3. *Oxt^{1-/-}* voles showed impairments in selective social motivation

(A) Operant lever pressing choice apparatuses for social and non-social choice contexts.

(B) WT females showed selective motivation for *peer* partners, whereas *Oxt^{1-/-}* females demonstrated no selective motivation.

(C) Both WT and *Oxt^{1-/-}* voles displayed selective motivation for their *mate* partner over the stranger.

(D) *Oxt^{1-/-}* animals showed no selective motivation to access the social (mate partner) over non-social (object) reward, in contrast to WT voles. *Oxt^{1-/-}* females worked significantly harder to access the novel object compared with WT females.

See analysis of behavioral interaction with reward stimulus in [Figure S2](#).

See statistics reported in [Table S3](#). * $p < 0.05$, ** $p < 0.01$, *** $p < 0.001$.

the eventual social attachment seen in partner preference tests was supported by environment and social experience. For instance, WT peer partners could facilitate relationship formation through social learning during cohabitation or testing. By using same-genotype cohorts of animals, we parsed out the effects of the *Oxt^{1-/-}* mutation from social learning or compensation by a WT partner, and the loss of selectivity became more obvious in this context. Although increased gregariousness may offer advantages such as broader social tolerance and reduced aggression, it may also come at the cost of stable relationships and potentially reduce fitness in environments where reliable social bonds support cooperative breeding or resource defense.

Furthermore, OXTRs are known to play an important role in both prosocial and antisocial behaviors in a region- and context-dependent manner.^{20,58–61} Deficits in social selectivity found in this assay may arise because the focal animal finds strangers more interesting (reduction in stranger avoidance), and/or because the animal finds its bonded partner less rewarding (reduced selective social reward) compared with WT individuals. These alternatives were assessed by interrogation of the role of OXTRs in selective social reward.

OXTRs are necessary for selective peer social reward

Social reward plays an important role in reinforcing social relationships.^{49,62,63} We found that *Oxt^{1-/-}* voles displayed impaired selective social motivation to access long-term peer partners but not mate partners. Moreover, although WT animals exhibited stronger motivation for social over non-social reward, *Oxt^{1-/-}* voles were motivated equally by both reward types

and worked harder to access the non-social reward than WT animals. These results suggest that OXTRs are not necessary for general reward learning and motivation but serve a more specific role in social reward and selective motivation for peer partners. Interestingly, intact reward selectivity in *Oxt^{1-/-}* voles in mate relationships may indicate that mate bonds are more robust and rewarding than peer bonds. Indeed, socially monogamous mate relationships are a key feature of the prairie vole mating system that contributes to reproductive success.⁶⁴

Overall, the loss of social selectivity in *Oxt^{1-/-}* prairie voles was a deficit observed across diverse ethological contexts, including dyadic and group interactions, various periods of relationship development, and multiple reward contexts, highlighting a critical role for OXTRs in effectively encoding peer relationships. Importantly, although there are no indications of impairments in parental care by OXTR null parents,³⁴ any life-long, constitutive loss of function inherently alters development. Future directions should explore how temporally and spatially precise manipulations of OXTRs in adulthood impact bond formation and selective attachment in peer relationships in a circuit-specific manner.

Loss of OXTR reduces levels of oxytocin release in the nucleus accumbens

Although loss of OXTR does not result in a compensatory increase in vasopressin receptor (V1aR) abundance,³⁴ it was unknown whether oxytocin release dynamics were altered in the absence of OXTR function. One possibility was that oxytocin synthesis and/or release is upregulated in compensation and signals through

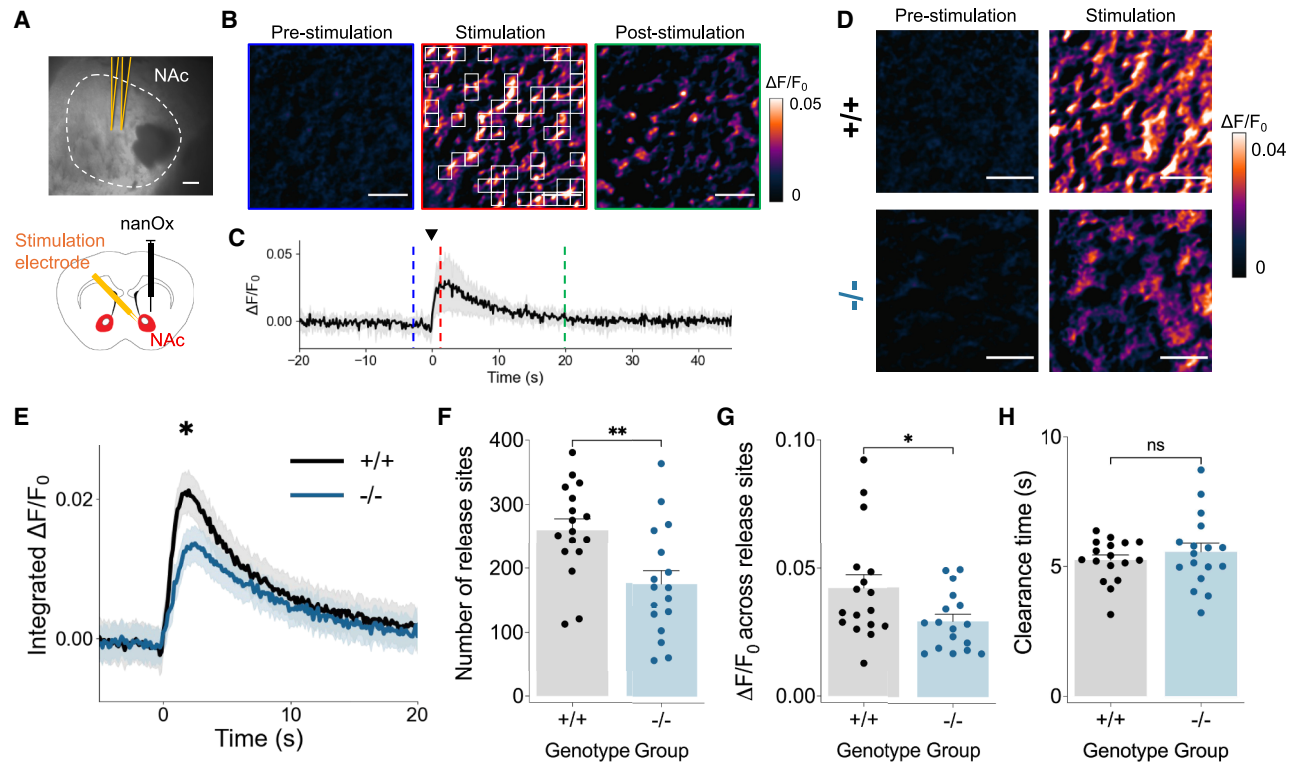


Figure 4. Fluorescence imaging with nanOx reveals reduced oxytocin signaling in the nucleus accumbens of *Oxt^{1-/-}* voles

(A) (Top) Bright-field image and (bottom) schematic showing the nucleus accumbens (NAc) in vole brain slices with stimulation electrodes (yellow). Scale bar represents 200 μm . The extracellular spaces of brain slices were labeled with nanOx (black).

(B) nanOx $\Delta F/F_0$ images in nucleus accumbens following 0.5 mA electrical stimulation in standard aCSF with 2 μM quinpirole. Three frames are shown: (left) “pre-stimulation” is the baseline $\Delta F/F_0$ before electrical stimulation; (center) “stimulation” is immediately after electrical stimulation, where a $6.8 \times 6.8 \mu\text{m}$ grid mask was applied and grids with high $\Delta F/F_0$ were identified as oxytocin release sites (white squares); and (right) “post-stimulation” is after $\Delta F/F_0$ has returned to baseline. Scale bars represent 20 μm .

(C) Time-course $\Delta F/F_0$ averaged over release sites in a single field of view ($175 \times 140 \mu\text{m}$) in the nucleus accumbens. The solid line is the averaged value of $\Delta F/F_0$ among identified release sites, and the shadow represents standard deviation (SD). Red, blue, and green dashed lines represent where pre-stimulation, stimulation, and post-stimulation images in (B) are taken from, respectively.

(D) $\Delta F/F_0$ images of nucleus accumbens (left) before and (right) upon stimulation (left) for (top) WT and (bottom) *Oxt^{1-/-}* voles. Scale bars represent 20 μm .

(E) Time-course of integrated $\Delta F/F_0$ in WT and *Oxt^{1-/-}* voles. The solid line is the averaged value and the shadow is SEM.

(F) The number of release sites identified in the field of view.

(G) $\Delta F/F_0$ over identified release sites.

(H) Oxytocin clearance time over identified release sites.

* $p < 0.05$, ** $p < 0.01$, *** $p < 0.001$, and **** $p < 0.0001$.

Error bar denotes the standard error of the mean.

See Figure S3 for details regarding nanOx sensor mechanisms and data processing.

See Figure S4 for evoked OXT (pre-quinpirole) and DA release.

See statistics reported in Table S4.

vasopressin V1a receptors to elicit similar downstream effects on social behavior. The nonpeptides oxytocin and vasopressin differ by only two of nine amino acids, allowing for substantial affinity at each other’s receptors.⁶⁵ Recent studies have noted instances in which these peptides act principally through these alternate pathways.^{16,19,65–71} Alternatively, oxytocin signaling could be downregulated in *Oxt^{1-/-}* voles due to the absence of functional receptors. Thus, we utilized nanOx nanosensors to understand how the *Oxt^{1-/-}* mutation may alter baseline physiological levels of oxytocin release with very high spatiotemporal resolution.

Interestingly, evoked oxytocin release was significantly reduced in the nucleus accumbens in *Oxt^{1-/-}* voles compared with WT animals, indicating that oxytocin release is

downregulated in the absence of OXTRs. Thus, relationship formation in the absence of OXTR is not accomplished by increased oxytocin acting at V1aR, at least in the nucleus accumbens. The reduction in oxytocin release in the absence of OXTR resulted both from a reduction in the number of oxytocin release sites and in the amount of oxytocin released from each site. The reduction in the number of oxytocin release sites may result from fewer oxytocinergic neurons or fewer oxytocinergic projections into the nucleus accumbens due to abnormal neural development. A recent study describing differences in the number of OXT-positive neurons in the paraventricular nucleus of the hypothalamus of *Oxt^{1-/-}* voles³⁵ supports this interpretation, though the mechanism underlying reduced oxytocin release remains

unclear and warrants further investigation. Overall, these results suggest positive feedback mechanisms in central oxytocin circuits, particularly in the absence of OXTRs, in line with previous findings that have proposed oxytocin engages in positive feedback on its own release.^{72–76}

Importantly, the coordinated actions of oxytocin and dopamine signaling in the nucleus accumbens reinforce various facets of social behavior across taxa.^{77,78} For instance, both oxytocin and dopamine are known to be major players in social behavior and mate pair-bonding in prairie voles.^{32,79–83} Recent studies in meadow voles have also demonstrated an association between greater evoked dopamine release and a social phenotype with greater OXTR density.^{84,85} The formation of selective peer social relationships in prairie voles appears not to be dependent on dopamine, although dopamine agonists can facilitate peer bonding,⁵⁷ and isolation from either a peer or a mate partner increases D1 receptor binding.^{57,86} Here, we found some indications that dopamine signaling in the nucleus accumbens is altered in *Oxtr*^{1–/–} prairie voles. Longer dopamine clearance time in mutant voles suggests potential changes in reuptake kinetics in the absence of OXTR that may be related to the phenotypic differences in social reward. Future studies are necessary to illuminate potential mechanisms of OXTR-modulation of dopamine dynamics in peer and mate relationship contexts.

OXTR deficit did not detectably alter body mass

We found that *Oxtr*^{1–/–} voles showed no increase in weight relative to controls. This finding differs from studies in OXTR and OXT knockout mice, which exhibit increased body weight and susceptibility to obesity.^{87,88} However, it is important to note that the discrepancy may arise from a difference in experimental timeline rather than a species-dependent effect. Genotype-dependent differences in body weight are commonly observed in late adulthood (post-natal day [P]85–120), while the present body weight data were collected at an early point of adulthood during behavioral testing (P60–80).

Conclusions

The present results underscore the role of OXTRs not only in facilitating the timely formation of selective peer relationships but also in maintaining the stability and selectivity of these bonds in broader social contexts. Alongside increased gregariousness observed in groups—characterized by rapid integration with novel conspecifics and loss of peer partner selectivity—*Oxtr*^{1–/–} voles also showed impairments in social reward, which may underlie their difficulty in maintaining stable, preferential peer relationships. This reduction in social reward, coupled with lower evoked oxytocin release in the nucleus accumbens, suggests that OXTR function is critical not just for forming attachments but also for sustaining the motivational salience of specific peer partners over time. Although increased gregariousness and indiscriminate social behavior may promote group cohesion or social flexibility in some contexts, these reductions in social selectivity may compromise the persistence of social bonds and have complex consequences for group dynamics and individual fitness in a socially monogamous and selective species. Together, these findings highlight how OXTR-dependent mechanisms shape the architecture of peer relationships and offer insight into understanding the neural mechanisms that support

selective sociality in humans, in whom close social relationships are foundational to mental health, well-being, and resilience.

RESOURCE AVAILABILITY

Lead contact

Further information and requests for resources and reagents should be directed to and will be fulfilled by the lead contact, Annaliese Beery (abeery@berkeley.edu).

Materials availability

nanOx and nIRCat nanosensors will be made available upon written request to M.P.L. (landry@berkeley.edu).

Data and code availability

- All data used to construct the figures in this study have been deposited at the Open Science Framework: <https://doi.org/10.17605/OSF.IO/QB7ZN>.
- This paper does not report original code.
- Any additional information required to reanalyze the data reported in this paper is available from the [lead contact](#) upon request.

ACKNOWLEDGMENTS

We appreciate Jaquesta Adams for nanOx sensor development; Antonella Alaco for assistance with behavioral testing and scoring; Jolyn Hoang for assistance with prairie vole genotyping; Alysha Batada, Nicole Chiang, Gautam Naik, and Stephan Song for assistance with operant training; Kelley Power for assistance with RFID protocols for apparatus setup and data acquisition; and UC Berkeley OLAC for routine animal care. We acknowledge the support of a National Science Foundation CAREER award 2239635 (A.K.B.), a National Institutes of Health grant R01MH132908 (A.K.B.), a Burroughs Wellcome Fund Career Award at the Scientific Interface (M.P.L. and N.K.), a Dreyfus Foundation Award (M.P.L.), the Philomathia Foundation (M.P.L.), an NSF CAREER award 2046159 (M.P.L.), McKnight Foundation award (M.P.L.), a Simons Foundation award (M.P.L.), a Moore Foundation award (M.P.L.), a Heising-Simons Fellowship (M.P.L.), a Brain Foundation award (M.P.L.), a Polymaths award from Schmidt Sciences, LLC (M.P.L.), and Schmidt Science Fellows, in partnership with the Rhodes Trust (N.K.). M.P.L. is a Chan Zuckerberg Biohub investigator.

AUTHOR CONTRIBUTIONS

A.M.B. and A.K.B. designed the experiments. A.M.B. performed the behavioral studies with assistance from J.Z. J.Z. and A.M.B. genotyped and reared voles. A.M.B., S.R.T., and N.S.S. scored behavioral videos and A.M.B. and A.K.B. analyzed corresponding data. N.K. and A.M.B. prepared *ex vivo* tissue, then N.K. performed all nanOx sensor experiments and analyzed imaging data. A.M.B., N.K., M.P.L., and A.K.B. wrote the manuscript. All authors discussed the results and commented on the manuscript.

DECLARATION OF INTERESTS

The authors declare no competing interest.

STAR★METHODS

Detailed methods are provided in the online version of this paper and include the following:

- [KEY RESOURCES TABLE](#)
- [EXPERIMENTAL MODEL AND STUDY PARTICIPANT DETAILS](#)
- [METHOD DETAILS](#)
 - Genotyping
 - Behavioral testing
 - Body weight and temperature
 - Near-infrared oxytocin imaging with nanOx nanosensors
- [QUANTIFICATION AND STATISTICAL ANALYSIS](#)

SUPPLEMENTAL INFORMATION

Supplemental information can be found online at <https://doi.org/10.1016/j.cub.2025.07.042>.

Received: May 14, 2025

Revised: July 10, 2025

Accepted: July 15, 2025

REFERENCES

- Grippe, A.J., Lamb, D.G., Carter, C.S., and Porges, S.W. (2007). Social Isolation Disrupts Autonomic Regulation of the Heart and Influences Negative Affective Behaviors. *Biol. Psychiatry* 62, 1162–1170. <https://doi.org/10.1016/j.biopsych.2007.04.011>.
- Holt-Lunstad, J., Smith, T.B., and Layton, J.B. (2010). Social Relationships and Mortality Risk: A Meta-analytic Review. *PLoS Med.* 7, e1000316. <https://doi.org/10.1371/journal.pmed.1000316>.
- Yang, Y.C., Boen, C., Gerken, K., Li, T., Schorpp, K., and Harris, K.M. (2016). Social relationships and physiological determinants of longevity across the human life span. *Proc. Natl. Acad. Sci. USA* 113, 578–583. <https://doi.org/10.1073/pnas.1511085112>.
- Mumtaz, F., Khan, M.I., Zubair, M., and Dehpour, A.R. (2018). Neurobiology and consequences of social isolation stress in animal model—A comprehensive review. *Biomed. Pharmacother.* 105, 1205–1222. <https://doi.org/10.1016/j.biopha.2018.05.086>.
- Snyder-Mackler, N., Burger, J.R., Gaydosh, L., Belsky, D.W., Noppert, G.A., Campos, F.A., Bartolomucci, A., Yang, Y.C., Aiello, A.E., O’Rand, A., et al. (2020). Social determinants of health and survival in humans and other animals. *Science* 368, eaax9553. <https://doi.org/10.1126/science.aax9553>.
- Neumann, I.D., and Slattery, D.A. (2016). Oxytocin in General Anxiety and Social Fear: A Translational Approach. *Biol. Psychiatry* 79, 213–221. <https://doi.org/10.1016/j.biopsych.2015.06.004>.
- Kupferberg, A., Bicks, L., and Hasler, G. (2016). Social functioning in major depressive disorder. *Neurosci. Biobehav. Rev.* 69, 313–332. <https://doi.org/10.1016/j.neubiorev.2016.07.002>.
- Brent, L.J.N., Chang, S.W.C., Gariépy, J.-F., and Platt, M.L. (2014). The neuroethology of friendship. *Ann. N. Y. Acad. Sci.* 1316, 1–17. <https://doi.org/10.1111/nyas.12315>.
- Massen, J., Sterck, E., and de Vos, H. (2010). Close social associations in animals and humans: functions and mechanisms of friendship. *Behaviour* 147, 1379–1412. <https://doi.org/10.1163/000579510X528224>.
- Olsen, R.B., Olsen, J., Gunner-Svensson, F., and Waldstrøm, B. (1991). Social networks and longevity. A 14 year follow-up study among elderly in Denmark. *Soc. Sci. Med.* 33, 1189–1195. [https://doi.org/10.1016/0277-9536\(91\)90235-5](https://doi.org/10.1016/0277-9536(91)90235-5).
- Bielsky, I.F., and Young, L.J. (2004). Oxytocin, vasopressin, and social recognition in mammals. *Peptides* 25, 1565–1574. <https://doi.org/10.1016/j.peptides.2004.05.019>.
- Young, L.J., and Wang, Z. (2004). The neurobiology of pair bonding. *Nat. Neurosci.* 7, 1048–1054. <https://doi.org/10.1038/nn1327>.
- Dölen, G. (2015). Autism: Oxytocin, serotonin, and social reward. *Soc. Neurosci.* 10, 450–465. <https://doi.org/10.1080/17470919.2015.1087875>.
- Insel, T.R., Winslow, J.T., Wang, Z., and Young, L.J. (1998). Oxytocin, Vasopressin, and the Neuroendocrine Basis of Pair Bond Formation. In *Vasopressin and Oxytocin: Molecular, Cellular, and Clinical Advances*, H.H. Zingg, C.W. Bourque, and D.G. Bichet, eds. (Springer), pp. 215–224. https://doi.org/10.1007/978-1-4615-4871-3_28.
- Anacker, A.M.J., and Beery, A.K. (2013). Life in groups: the roles of oxytocin in mammalian sociality. *Front. Behav. Neurosci.* 7, 185. <https://doi.org/10.3389/fnbeh.2013.00185>.
- Rigney, N., De Vries, G.J., Petrusis, A., and Young, L.J. (2022). Oxytocin, Vasopressin, and Social Behavior: From Neural Circuits to Clinical Opportunities. *Endocrinology* 163, bqac111. <https://doi.org/10.1210/en-docr/bqac111>.
- Jurek, B., and Neumann, I.D. (2018). The Oxytocin Receptor: From Intracellular Signaling to Behavior. *Physiol. Rev.* 98, 1805–1908. <https://doi.org/10.1152/physrev.00031.2017>.
- Beery, A.K., and Zucker, I. (2010). Oxytocin and same-sex social behavior in female meadow voles. *Neuroscience* 169, 665–673. <https://doi.org/10.1016/j.neuroscience.2010.05.023>.
- Anacker, A.M.J., Christensen, J.D., LaFlamme, E.M., Grunberg, D.M., and Beery, A.K. (2016). Septal oxytocin administration impairs peer affiliation via V1a receptors in female meadow voles. *Psychoneuroendocrinology* 68, 156–162. <https://doi.org/10.1016/j.psychneuen.2016.02.025>.
- Beery, A.K., Lopez, S.A., Blandino, K.L., Lee, N.S., and Bourdon, N.S. (2021). Social selectivity and social motivation in voles. *eLife* 10, e72684. <https://doi.org/10.7554/eLife.72684>.
- Carter, C.S., and Getz, L.L. (1993). Monogamy and the Prairie Vole. *Sci. Am.* 268, 100–106. <https://doi.org/10.1038/scientificamerican0693-100>.
- McGraw, L.A., and Young, L.J. (2010). The prairie vole: an emerging model organism for understanding the social brain. *Trends Neurosci.* 33, 103–109. <https://doi.org/10.1016/j.tins.2009.11.006>.
- Kenkel, W.M., Gustison, M.L., and Beery, A.K. (2021). A Neuroscientist’s Guide to the Vole. *Curr. Protoc.* 1, e175. <https://doi.org/10.1002/cpz1.175>.
- Schweinfurth, M.K., Neuenschwander, J., Engqvist, L., Schneeberger, K., Rentsch, A.K., Gyax, M., and Taborsky, M. (2017). Do female Norway rats form social bonds? *Behav. Ecol. Sociobiol.* 71, 98. <https://doi.org/10.1007/s00265-017-2324-2>.
- Beery, A.K., and Shambaugh, K.L. (2021). Comparative Assessment of Familiarity/Novelty Preferences in Rodents. *Front. Behav. Neurosci.* 15, 648830. <https://doi.org/10.3389/fnbeh.2021.648830>.
- Lee, N.S., Goodwin, N.L., Freitas, K.E., and Beery, A.K. (2019). Affiliation, Aggression, and Selectivity of Peer Relationships in Meadow and Prairie Voles. *Front. Behav. Neurosci.* 13, 52. <https://doi.org/10.3389/fnbeh.2019.00052>.
- Carter, C.S., DeVries, A.C., and Getz, L.L. (1995). Physiological substrates of mammalian monogamy: The prairie vole model. *Neurosci. Biobehav. Rev.* 19, 303–314. [https://doi.org/10.1016/0149-7634\(94\)00070-H](https://doi.org/10.1016/0149-7634(94)00070-H).
- Johnson, Z.V., Walum, H., Jamal, Y.A., Xiao, Y., Keebaugh, A.C., Inoue, K., and Young, L.J. (2016). Central oxytocin receptors mediate mating-induced partner preferences and enhance correlated activation across forebrain nuclei in male prairie voles. *Horm. Behav.* 79, 8–17. <https://doi.org/10.1016/j.yhbeh.2015.11.011>.
- Cho, M.M., DeVries, A.C., Williams, J.R., and Carter, C.S. (1999). The effects of oxytocin and vasopressin on partner preferences in male and female prairie voles (*Microtus ochrogaster*). *Behav. Neurosci.* 113, 1071–1079. <https://doi.org/10.1037/0735-7044.113.5.1071>.
- Williams, J.R., Insel, T.R., Harbaugh, C.R., and Carter, C.S. (1994). Oxytocin administered centrally facilitates formation of a partner preference in female prairie voles (*Microtus ochrogaster*). *J. Neuroendocrinol.* 6, 247–250. <https://doi.org/10.1111/j.1365-2826.1994.tb00579.x>.
- DeVries, A.C., Johnson, C.L., and Carter, C.S. (1997). Familiarity and gender influence social preferences in prairie voles (*Microtus ochrogaster*). *Can. J. Zool.* 75, 295–301. <https://doi.org/10.1139/z97-037>.
- Liu, Y., and Wang, Z.X. (2003). Nucleus accumbens oxytocin and dopamine interact to regulate pair bond formation in female prairie voles. *Neuroscience* 121, 537–544. [https://doi.org/10.1016/S0306-4522\(03\)00555-4](https://doi.org/10.1016/S0306-4522(03)00555-4).
- Young, L.J., Lim, M.M., Gingrich, B., and Insel, T.R. (2001). Cellular Mechanisms of Social Attachment. *Horm. Behav.* 40, 133–138. <https://doi.org/10.1006/hbeh.2001.1691>.
- Berendzen, K.M., Sharma, R., Mandujano, M.A., Wei, Y., Rogers, F.D., Simmons, T.C., Seelke, A.M.H., Bond, J.M., Larios, R., Goodwin, N.L., et al. (2023). Oxytocin receptor is not required for social attachment in

- prairie voles. *Neuron* 111, 787–796.e4. <https://doi.org/10.1016/j.neuron.2022.12.011>.
35. Sharma, R., Berendzen, K.M., Everitt, A., Wang, B., Williams, G., Wang, S., Quine, K., Larios, R.D., Long, K.L.P., Hoglen, N., et al. (2024). Oxytocin receptor controls distinct components of pair bonding and development in prairie voles. Preprint at bioRxiv. <https://doi.org/10.1101/2024.09.25.613753>.
 36. Shamay-Tsoory, S.G., and Abu-Akel, A. (2016). The Social Salience Hypothesis of Oxytocin. *Biol. Psychiatry* 79, 194–202. <https://doi.org/10.1016/j.biopsych.2015.07.020>.
 37. Wolf, D., Hartig, R., Zhuo, Y., Scheller, M.F., Articus, M., Moor, M., Grinevich, V., Linster, C., Russo, E., Weber-Fahr, W., et al. (2024). Oxytocin induces the formation of distinctive cortical representations and cognitions biased toward familiar mice. *Nat. Commun.* 15, 6274. <https://doi.org/10.1038/s41467-024-50113-6>.
 38. Marlin, B.J., Mitre, M., D'amour, J.A., Chao, M.V., and Froemke, R.C. (2015). Oxytocin enables maternal behaviour by balancing cortical inhibition. *Nature* 520, 499–504. <https://doi.org/10.1038/nature14402>.
 39. Goodwin, N.L., Lopez, S.A., Lee, N.S., and Beery, A.K. (2019). Comparative role of reward in long-term peer and mate relationships in voles. *Horm. Behav.* 111, 70–77. <https://doi.org/10.1016/j.yhbeh.2018.10.012>.
 40. Vahaba, D.M., Halstead, E.R., Donaldson, Z.R., Ahern, T.H., and Beery, A.K. (2022). Sex differences in the reward value of familiar mates in prairie voles. *Genes Brain Behav.* 21, e12790. <https://doi.org/10.1111/gbb.12790>.
 41. Brusman, L.E., Protter, D.S.W., Fultz, A.C., Paulson, M.U., Chapel, G.D., Elges, I.O., Cameron, R.T., Beery, A.K., and Donaldson, Z.R. (2022). Emergent intra-pair sex differences and organized behavior in pair bonded prairie voles (*Microtus ochrogaster*). *Genes Brain Behav.* 21, e12786. <https://doi.org/10.1111/gbb.12786>.
 42. Soergel D.A. and Beery A.K. (2024). Voletron (Version 1.0.0). <https://github.com/BeeryLab/voletron>.
 43. Power, K.C., Lee, N.S., Rendon-Torres, K., Soergel, D.A.W., and Beery, A.K. (2025). A social switch: daylength drives meadow vole group dynamics in automatically tracked habitats. *Anim. Behav.* 222, 123084. <https://doi.org/10.1016/j.anbehav.2025.123084>.
 44. Adams, J.A.M., Komatsu, N., Navarro, N., Black, A.M., Leem, E., Sun, X., Zhao, J., Arias-Soto, O.I., Beery, A.K., and Landry, M.P. (2025). High-throughput evolution of near-infrared oxytocin nanosensors enables oxytocin imaging in mice and prairie voles. Preprint at bioRxiv. <https://doi.org/10.1101/2024.05.10.593556>.
 45. Piekarski, D.J., Boivin, J.R., and Wilbrecht, L. (2017). Ovarian Hormones Organize the Maturation of Inhibitory Neurotransmission in the Frontal Cortex at Puberty Onset in Female Mice. *Curr. Biol.* 27, 1735–1745.e3. <https://doi.org/10.1016/j.cub.2017.05.027>.
 46. Yang, S.J., Del Bonis-O'Donnell, J.T., Beyene, A.G., and Landry, M.P. (2021). Near-infrared catecholamine nanosensors for high spatiotemporal dopamine imaging. *Nat. Protoc.* 16, 3026–3048. <https://doi.org/10.1038/s41596-021-00530-4>.
 47. Beyene, A.G., Delevich, K., Del Bonis-O'Donnell, J.T., Piekarski, D.J., Lin, W.C., Thomas, A.W., Yang, S.J., Kosillo, P., Yang, D., Prounis, G.S., et al. (2019). Imaging striatal dopamine release using a nongenetically encoded near infrared fluorescent catecholamine nanosensor. *Sci. Adv.* 5, eaaw3108. <https://doi.org/10.1126/sciadv.aaw3108>.
 48. Xiao, L., Priest, M.F., Nasenbeny, J., Lu, T., and Kozorovitskiy, Y. (2017). Biased Oxytocinergic Modulation of Midbrain Dopamine Systems. *Neuron* 95, 368–384.e5. <https://doi.org/10.1016/j.neuron.2017.06.003>.
 49. Hung, L.W., Neuner, S., Polepalli, J.S., Beier, K.T., Wright, M., Walsh, J.J., Lewis, E.M., Luo, L., Deisseroth, K., Dölen, G., et al. (2017). Gating of social reward by oxytocin in the ventral tegmental area. *Science* 357, 1406–1411. <https://doi.org/10.1126/science.aan4994>.
 50. Briffaud, V., Williams, P., Courty, J., and Broberger, C. (2015). Excitation of Tuberoinfundibular Dopamine Neurons by Oxytocin: Crosstalk in the Control of Lactation. *J. Neurosci.* 35, 4229–4237. <https://doi.org/10.1523/JNEUROSCI.2633-14.2015>.
 51. Shahrokh, D.K., Zhang, T.-Y., Diorio, J., Gratton, A., and Meaney, M.J. (2010). Oxytocin-dopamine interactions mediate variations in maternal behavior in the rat. *Endocrinology* 151, 2276–2286. <https://doi.org/10.1210/en.2009-1271>.
 52. Love, T.M. (2014). Oxytocin, motivation and the role of dopamine. *Pharmacol. Biochem. Behav.* 119, 49–60. <https://doi.org/10.1016/j.pbb.2013.06.011>.
 53. Lee, N.S., and Beery, A.K. (2021). The role of dopamine signaling in prairie vole peer relationships. *Horm. Behav.* 127, 104876. <https://doi.org/10.1016/j.yhbeh.2020.104876>.
 54. Liu, Y., Curtis, J.T., and Wang, Z. (2001). Vasopressin in the lateral septum regulates pair bond formation in male prairie voles (*Microtus ochrogaster*). *Behav. Neurosci.* 115, 910–919. <https://doi.org/10.1037//0735-7044.115.4.910>.
 55. Johnson, Z.V., Walum, H., Xiao, Y., Riefkohl, P.C., and Young, L.J. (2017). Oxytocin receptors modulate a social salience neural network in male prairie voles. *Horm. Behav.* 87, 16–24. <https://doi.org/10.1016/j.yhbeh.2016.10.009>.
 56. Donaldson, Z.R., and Young, L.J. (2008). Oxytocin, Vasopressin, and the Neurogenetics of Sociality. *Science* 322, 900–904. <https://doi.org/10.1126/science.1158668>.
 57. Lee, N.S., Kim, C.Y., and Beery, A.K. (2023). Peer Social Environment Impacts Behavior and Dopamine D1 Receptor Density in Prairie Voles (*Microtus ochrogaster*). *Neuroscience* 515, 62–70. <https://doi.org/10.1016/j.neuroscience.2023.02.002>.
 58. Beery, A.K. (2015). Antisocial oxytocin: complex effects on social behavior. *Curr. Opin. Behav. Sci.* 6, 174–182. <https://doi.org/10.1016/j.cobeha.2015.11.006>.
 59. Guzmán, Y.F., Tronson, N.C., Jovasevic, V., Sato, K., Guedea, A.L., Mizukami, H., Nishimori, K., and Radulovic, J. (2013). Fear-enhancing effects of septal oxytocin receptors. *Nat. Neurosci.* 16, 1185–1187. <https://doi.org/10.1038/nn.3465>.
 60. Martinon, D., Lis, P., Roman, A.N., Tornesi, P., Applebey, S.V., Buechner, G., Olivera, V., and Dabrowska, J. (2019). Oxytocin receptors in the dorso-lateral bed nucleus of the stria terminalis (BNST) bias fear learning toward temporally predictable cued fear. *Transl. Psychiatry* 9, 140. <https://doi.org/10.1038/s41398-019-0474-x>.
 61. Olazábal, D.E., and Young, L.J. (2006). Species and individual differences in juvenile female alloparental care are associated with oxytocin receptor density in the striatum and the lateral septum. *Horm. Behav.* 49, 681–687. <https://doi.org/10.1016/j.yhbeh.2005.12.010>.
 62. Dölen, G., Darvishzadeh, A., Huang, K.W., and Malenka, R.C. (2013). Social reward requires coordinated activity of nucleus accumbens oxytocin and serotonin. *Nature* 501, 179–184. <https://doi.org/10.1038/nature12518>.
 63. Borland, J.M., Rilling, J.K., Frantz, K.J., and Albers, H.E. (2019). Sex-dependent regulation of social reward by oxytocin: an inverted U hypothesis. *Neuropsychopharmacology* 44, 97–110. <https://doi.org/10.1038/s41386-018-0129-2>.
 64. Ophir, A.G., Phelps, S.M., Sorin, A.B., and Wolff, J.O. (2008). Social but not genetic monogamy is associated with greater breeding success in prairie voles. *Anim. Behav.* 75, 1143–1154. <https://doi.org/10.1016/j.anbehav.2007.09.022>.
 65. Rae, M., Lemos Duarte, M., Gomes, I., Camarini, R., and Devi, L.A. (2022). Oxytocin and vasopressin: Signalling, behavioural modulation and potential therapeutic effects. *Br. J. Pharmacol.* (Wiley Online Library) 179, 1544–1564. <https://doi.org/10.1111/bph.15481>.
 66. Sala, M., Braidà, D., Lentini, D., Busnelli, M., Bulgheroni, E., Capurro, V., Finardi, A., Donzelli, A., Pattini, L., Rubino, T., et al. (2011). Pharmacologic Rescue of Impaired Cognitive Flexibility, Social Deficits, Increased Aggression, and Seizure Susceptibility in Oxytocin Receptor Null

- Mice: A Neurobehavioral Model of Autism. *Biol. Psychiatry* 69, 875–882. <https://doi.org/10.1016/j.biopsych.2010.12.022>.
67. Song, Z., McCann, K.E., McNeill, J.K., Larkin, T.E., Huhman, K.L., and Albers, H.E. (2014). Oxytocin induces social communication by activating arginine-vasopressin V1a receptors and not oxytocin receptors. *Psychoneuroendocrinology* 50, 14–19. <https://doi.org/10.1016/j.psypneuen.2014.08.005>.
68. Smith, C.J.W., DiBenedictis, B.T., and Veenema, A.H. (2019). Comparing vasopressin and oxytocin fiber and receptor density patterns in the social behavior neural network: Implications for cross-system signaling. *Front. Neuroendocrinol.* 53, 100737. <https://doi.org/10.1016/j.yfrne.2019.02.001>.
69. Song, Z., and Albers, H.E. (2018). Cross-talk among oxytocin and arginine-vasopressin receptors: Relevance for basic and clinical studies of the brain and periphery. *Front. Neuroendocrinol.* 51, 14–24. <https://doi.org/10.1016/j.yfrne.2017.10.004>.
70. Qiu, F., Qiu, C.-Y., Cai, H., Liu, T.-T., Qu, Z.-W., Yang, Z., Li, J.-D., Zhou, Q.-Y., and Hu, W.-P. (2014). Oxytocin inhibits the activity of acid-sensing ion channels through the vasopressin, V1A receptor in primary sensory neurons. *Br. J. Pharmacol.* 171, 3065–3076. <https://doi.org/10.1111/bph.12635>.
71. Schorscher-Petcu, A., Sotocinal, S., Ciura, S., Dupré, A., Ritchie, J., Sorge, R.E., Crawley, J.N., Hu, S.-B., Nishimori, K., Young, L.J., et al. (2010). Oxytocin-Induced Analgesia and Scratching Are Mediated by the Vasopressin-1A Receptor in the Mouse. *J. Neurosci.* 30, 8274–8284. <https://doi.org/10.1523/JNEUROSCI.1594-10.2010>.
72. Yamashita, H., Okuya, S., Inenaga, K., Kasai, M., Uesugi, S., Kannan, H., and Kaneko, T. (1987). Oxytocin predominantly excites putative oxytocin neurons in the rat supraoptic nucleus in vitro. *Brain Res.* 416, 364–368. [https://doi.org/10.1016/0006-8993\(87\)90920-6](https://doi.org/10.1016/0006-8993(87)90920-6).
73. Moos, F., and Richard, P. (1989). Paraventricular and supraoptic bursting oxytocin cells in rat are locally regulated by oxytocin and functionally related. *J. Physiol.* 408, 1–18. <https://doi.org/10.1113/jphysiol.1989.sp017442>.
74. Moos, F., Freund-Mercier, M.J., Guerné, Y., Guerné, J.M., Stoeckel, M.E., and Richard, P. (1984). Release of oxytocin and vasopressin by magnocellular nuclei in vitro: specific facilitatory effect of oxytocin on its own release. *J. Endocrinol.* 102, 63–72. <https://doi.org/10.1677/joe.0.1020063>.
75. Neumann, I., Douglas, A.J., Pittman, Q.J., Russell, J.A., and Landgraf, R. (1996). Oxytocin Released within the Supraoptic Nucleus of the Rat Brain by Positive Feedback Action is Involved in Parturition-Related Events. *J. Neuroendocrinol.* 8, 227–233. <https://doi.org/10.1046/j.1365-2826.1996.04557.x>.
76. Hatton, G.I. (1990). Emerging concepts of structure-function dynamics in adult brain: The hypothalamo-neurohypophysial system. *Prog. Neurobiol.* 34, 437–504. [https://doi.org/10.1016/0301-0082\(90\)90017-B](https://doi.org/10.1016/0301-0082(90)90017-B).
77. Rappeneau, V., and Castillo Díaz, F. (2024). Convergence of oxytocin and dopamine signalling in neuronal circuits: Insights into the neurobiology of social interactions across species. *Neurosci. Biobehav. Rev.* 161, 105675. <https://doi.org/10.1016/j.neubiorev.2024.105675>.
78. Castillo Díaz, F.C., Neumann, I.D., and Rappeneau, V. (2025). Oxytocin and dopamine in psychostimulant-induced changes in social behaviour. *Front. Neuroendocrinol.* 78, 101200. <https://doi.org/10.1016/j.yfrne.2025.101200>.
79. Resendez, S.L., Keyes, P.C., Day, J.J., Hambro, C., Austin, C.J., Maina, F.K., Eidson, L.N., Porter-Stransky, K.A., Nevárez, N., McLean, J.W., et al. (2016). Dopamine and opioid systems interact within the nucleus accumbens to maintain monogamous pair bonds. *eLife* 5, e15325. <https://doi.org/10.7554/eLife.15325>.
80. Loth, M.K., and Donaldson, Z.R. (2021). Oxytocin, Dopamine, and Opioid Interactions Underlying Pair Bonding: Highlighting a Potential Role for Microglia. *Endocrinology* 162, bqaa223. <https://doi.org/10.1210/endo/bqaa223>.
81. Aragona, B.J., Liu, Y., Curtis, J.T., Stephan, F.K., and Wang, Z. (2003). A Critical Role for Nucleus Accumbens Dopamine in Partner-Preference Formation in Male Prairie Voles. *J. Neurosci.* 23, 3483–3490. <https://doi.org/10.1523/JNEUROSCI.23-08-03483.2003>.
82. Zhang, L., Qu, Y., Li, L., Sun, Y., Qian, W., Xiao, J., Huang, K., Han, X., Niu, H., Li, L., et al. (2025). PVN–NAC Shell–VP Circuit OT and OTR Neurons Regulate Pair Bonding via D2R and D1R. *J. Neurosci.* 45, e2061242025. <https://doi.org/10.1523/JNEUROSCI.2061-24.2025>.
83. Pierce, A.F., Protter, D.S.W., Watanabe, Y.L., Chapel, G.D., Cameron, R.T., and Donaldson, Z.R. (2024). Nucleus accumbens dopamine release reflects the selective nature of pair bonds. *Curr. Biol.* 34, 519–530.e5. <https://doi.org/10.1016/j.cub.2023.12.041>.
84. Beery, A.K. (2019). Frank Beach award winner: Neuroendocrinology of group living. *Horm. Behav.* 107, 67–75. <https://doi.org/10.1016/j.yhbeh.2018.11.002>.
85. Mun, J., Power, K.C., Beery, A.K., and Landry, M.P. (2025). Neurochemical imaging reveals changes in dopamine dynamics with photoperiod in a seasonally social vole species. Preprint at bioRxiv. <https://doi.org/10.1101/2025.05.11.652581>.
86. Vitale, E.M., Kirckof, A., and Smith, A.S. (2023). Partner-seeking and limbic dopamine system are enhanced following social loss in male prairie voles (*Microtus ochrogaster*). *Genes Brain Behav.* 22, e12861. <https://doi.org/10.1111/gbb.12861>.
87. Takayanagi, Y., Kasahara, Y., Onaka, T., Takahashi, N., Kawada, T., and Nishimori, K. (2008). Oxytocin receptor-deficient mice developed late-onset obesity. *NeuroReport* 19, 951–955. <https://doi.org/10.1097/WNR.0b013e3283021ca9>.
88. Camerino, C. (2009). Low Sympathetic Tone and Obese Phenotype in Oxytocin-deficient Mice. *Obesity (Silver Spring)* 17, 980–984. <https://doi.org/10.1038/oby.2009.12>.
89. Pérez-Escudero, A., Vicente-Page, J., Hinz, R.C., Arganda, S., and de Polavieja, G.G. (2014). idTracker: tracking individuals in a group by automatic identification of unmarked animals. *Nat. Methods* 11, 743–748. <https://doi.org/10.1038/nmeth.2994>.
90. Edelstein, A.D., Tsuchida, M.A., Amodaj, N., Pinkard, H., Vale, R.D., and Stuurman, N. (2014). Advanced methods of microscope control using µManager software. *J. Biol. Methods* 1, e10. <https://doi.org/10.14440/jbm.2014.36>.
91. Schindelin, J., Arganda-Carreras, I., Frise, E., Kaynig, V., Longair, M., Pietzsch, T., Preibisch, S., Rueden, C., Saalfeld, S., Schmid, B., et al. (2012). Fiji: an open-source platform for biological-image analysis. *Nat. Methods* 9, 676–682. <https://doi.org/10.1038/nmeth.2019>.
92. Mun, J., Navarro, N., Jeong, S., Ouassil, N., Leem, E., Beyene, A.G., and Landry, M.P. (2024). Near-infrared nanosensors enable optical imaging of oxytocin with selectivity over vasopressin in acute mouse brain slices. *Proc. Natl. Acad. Sci. USA* 121, e2314795121. <https://doi.org/10.1073/pnas.2314795121>.
93. Ahern, T.H., Modi, M.E., Burkett, J.P., and Young, L.J. (2009). Evaluation of two automated metrics for analyzing partner preference tests. *J. Neurosci. Methods* 182, 180–188. <https://doi.org/10.1016/j.jneumeth.2009.06.010>.
94. Beery, A.K. (2021). Familiarity and Mate Preference Assessment with the Partner Preference Test. *Curr. Protoc.* 1, e173. <https://doi.org/10.1002/cpz1.173>.

STAR★METHODS

KEY RESOURCES TABLE

REAGENT or RESOURCE	SOURCE	IDENTIFIER
Chemicals, peptides, and recombinant proteins		
HiPco Small Diameter SWCNTs	NanoIntegrals	HiPco Raw SWNTs
Sodium chloride	Sigma-Aldrich	S3014; CAS7647-14-5
Sodium bicarbonate	Sigma-Aldrich	S6014; CAS144-55-8
Potassium chloride	Sigma-Aldrich	P9333; CAS 7447-40-7
Sodium phosphate monobasic	Sigma-Aldrich	S8282; CAS7558-80-7
Magnesium Chloride	Quality Biological	351-033-721
Calcium chloride	VWR	E506; CAS10035-04-8
D-(+)-Glucose	Sigma-Aldrich	G7528; CAS50-99-7
Oxygen/carbon dioxide (95% O ₂ , 5% CO ₂ ; carbogen)	Praxair	cat. no. BIOXCD5C-K
Isoflurane	Sigma-Aldrich	CAS 26675-46-7
Ketamine Hydrochloride Injection	Dechra	CAS 1867-66-9
Xylazine		
(-)-Quinpirole hydrochloride, Tocris Bioscience™	Fisher Scientific	10-611-0; CAS 85798-08-9
Proteinase K, recombinant PCR grade	Roche Diagnostic	03115879001
XcmI restriction enzyme	New England Biolabs	NEB# R0533S
Critical commercial assays		
Qiagen DNEasy kit	Qiagen	Cat# 69504
Taq PCR Core Kit	Qiagen	Cat# 201223
Deposited data		
Data for figure panels	This paper	OSF: https://doi.org/10.17605/OSF.IO/QB7ZN
Experimental models: Organisms/strains		
<i>Oxtr</i> ^{1-/-} mutant prairie vole	Berendzen et al. ³⁴	<i>Oxtr</i> ^{1-/-}
Wildtype prairie vole (<i>Microtus ochrogaster</i>)	This paper	N/A
Oligonucleotides		
OXTR forward primer: ACTGGAGCTTCGAGTTGGAC	Integrated DNA technologies (IDT)	N/A
OXTR reverse primer: ATGCCACCACTTGCAAGTA	Integrated DNA technologies (IDT)	N/A
ssDNA for NaoOx nanosensor: CCCCCACGGGACCGCAGATCGAGCCCCC	Integrated DNA technologies (IDT)	N/A
Software and algorithms		
Voletron 1.0	Github voletron	https://github.com/BeeryLab/voletron
idTracker	Pérez-Escudero et al. ⁸⁹	https://www.idtracker.es/
ClockLab	ActiMetrics	https://actimetrics.com/products/clocklab/clocklab-analysis-version-6/
OLCUS	FBI-Science GmbH	https://fbiscience.com/wp/index.php/en/olcus-3/
MED-PC VI	Med Associates	https://med-associates.com/product/med-pc/
InterVole Timer	Github intervole_timer	https://github.com/BeeryLab/intervole_timer
GraphPad Prism (Version 10)	GraphPad Software	https://graphpad.com/scientificsoftware/prism/
JMP Pro (Version 17)	JMP Statistical Discovery	https://www.jmp.com/en/software
Micro-Manager	Edelstein et al. ⁹⁰	https://www.micro-manager.org
Fiji	Schindelin et al. ⁹¹	https://imagej.net/Fiji
Image processing algorithm	Mun et al. ⁹²	https://github.com/NicholasOuassil/NanolmgPro

(Continued on next page)

Continued

REAGENT or RESOURCE	SOURCE	IDENTIFIER
Other		
Habitat tracking PIT tag	Biomark	APT12 FDX-B
Temperature PIT tag	Biomark	BioTherm13 FDX-B
3-chamber modular operant apparatus	Med Associates	ENV-307A
Ultrasonic homogenizer with 6-mm tip	Cole-Parmer	UX-04711-70 and UX-04712-14
Microvolume UV-Vis Spectrophotometer	Thermo Scientific	NanoDrop One
Vibrating blade microtome, vibratome	Leica	VT1200
Microtome razor blades	Personna	double edge super blades
Slice incubation chamber	Scientific Systems Design, Inc.	BSK4
Low-volume slice incubation chamber	Scientific Systems Design, Inc.	BSK2
785-nm CW diode laser	OptoEngine LLC	MDL-III-785R-300mW
nIR InGaAs camera	Raptor Photonics	Ninox 640
Perfusion pump	World Precision Instruments	Peri-Star Pro
Aspirator pump	Warner Instruments	Dedicated Workstation Vacuum System
Inline heater with feedback control	Warner Instruments	TV-324C
Bipolar stimulation electrode	MicroProbes for Life Science	PI2ST30.1A5
4X objective	Olympus	XLFluor 4X/340
60X objective	Nikon	CFI Apochromat NIR 60X W

EXPERIMENTAL MODEL AND STUDY PARTICIPANT DETAILS

Wildtype and *Oxtr*^{1-/-} female prairie voles were bred in-house in a long photoperiod (14 hr light:10 hr dark; lights off at 18:00 PST). All breeding pairs were previously outcrossed for 7 generations per standard genetic protocols. Wildtype focal animals were derived from a wildtype father and a wildtype or heterozygous mother, while *Oxtr*^{1-/-} voles were born from a heterozygous or homozygous *Oxtr*^{1-/-} father and a heterozygous mother. Parental genotype in this line has previously been shown not to affect parental care,³⁴ but homozygous *Oxtr*^{1-/-} females were never used in a breeding pair due to the importance of OXTRs in parturition and nursing. Voles were weaned and genotyped at postnatal day (PND) 21 and then separated into same-sex pairs in clear plastic cages with sani-chip bedding and an opaque plastic hiding tube by PND 28. In adulthood (PND 5080), voles were randomly assigned to one of the three social behavior testing paradigms before use in the oxytocin imaging portion of the study (PND 80-100). There were no significant effects of behavioral testing history on oxytocin release in the imaging experiment.

Only female voles were used to study peer relationships because male prairie voles can show lethal levels of aggression when co-housed with novel, same-sex individuals in adulthood.²⁶ Furthermore, female peer relationships are more ethologically relevant and are commonly observed in wild prairie voles in contexts such as spontaneous alloparental care.⁶¹ Therefore, experiments that included re-pairing or cohabitation with novel, same-sex animals were restricted to the use of female voles due to animal welfare concerns and interest in biological application to natural social behavior. Both male and female subjects were included in the oxytocin and dopamine imaging experiments to assess possible sex differences in neural signaling. All procedures adhered to federal and institutional guidelines and were approved by the Institutional Animal Care and Use Committee at the University of California, Berkeley.

METHOD DETAILS

Genotyping

We collected 1 mm tail samples from animals anesthetized with isoflurane. Tissue samples were lysed according to methods published in Berendzene et al.³⁴ In short, 200 μ L of tail lysis buffer and 10 μ L of proteinase K were added to each tube and left to incubate at 56 °C overnight (18–24 hours). Following incubation, samples were briefly spun down and then placed in a 95 °C heat block for 20 minutes to inactivate proteinase K. DNA was subsequently isolated using the Qiagen DNeasy Blood & Tissue Kit, and DNA concentration was quantified using a Nanodrop spectrophotometer. Next, we used polymerase chain reaction and restriction enzyme digestion (Qiagen Taq PCR core kit; XcmI) to establish genotypes according to published protocols (Berendzen et al.³⁴). Digested DNA was run on a 2% agarose gel containing SYBR Safe dye in 1X TBE buffer at 140 volts for 45 minutes. The resulting bands were visualized using an Azure Biosystems gel imager.

Behavioral testing

Partner preference test (PPT)

Peer PPTs were carried out using a linear 3-chamber apparatus (Figure 1A) according to previously established methods for preference testing.^{93,94} Each behavioral test was recorded and analyzed using automated tracking (idTracker) and scored by a blind observer with custom software (Intervole Timer v1.6; https://github.com/BeeryLab/intervole_timer). We tested the accuracy of automated scoring by comparing it to data from manual scoring on a subset of behavioral tests and found no difference between the two methods in chamber time or huddling time metrics (*Chamber time*: $R^2 = 0.9933$, $F(1, 7) = 1031$, $p < .0001$; *Huddling time*: $R^2 = 0.7484$, $F(1, 6) = 17.84$, $p < .0055$). Aggressive bouts were manually scored during the first 20 minutes of recorded tests (PPT 1-3).

In early adulthood (PND 50-70), focal females were tested in the first PPT with a lifetime partner where they had the choice between interacting with a novel “stranger” vole and familiar cagemate “partner” during the 180-minute test. Afterward, each focal vole was separated for three days to prevent aggression upon re-pairing, then placed with a new peer partner for 24-hour cohabitation before the second PPT. Finally, after a week of cohabitation with the new peer partner, the focal females were tested in a third PPT to assess changes in bond formation.

Radio-frequency identification (RFID) tracking

Free-moving group social dynamics were tracked using RFID tags over a week of undisturbed cohabitation. The group-living habitat is an apparatus composed of five interconnected chambers as previously described by our group.⁴³ Each chamber is connected by clear acrylic tubes equipped with ring antennas on each side to provide positional tracking of each vole as it moves throughout the habitat. For RFID analysis, raw positional data were collected and processed with Voletron 1.0 (<https://github.com/BeeryLab/voletron>). Data were analyzed in hour increments for the first three hours and 24-hour intervals across the six days of testing. Social preferences were quantified as time spent with the partner in any size of group/all social time and compared between genotype groups. Each group was also compared to the expected value for partner cohabitation at random (“expected random”), i.e. if no familiarity preference existed. Expected random values depend on the amount of time individual animals spent in groups of different sizes, as well as the probability of being with the partner by chance in each of those group combinations (i.e. one of three possible pairs involve the partner, two of three possible trios involve the partner, and all possible quads involve the partner). Thus, for each individual, the expected random time with the partner = ($1/3$ *time in pairs)+(2/3*time in trios)+(1*time in quad). These values were averaged across individuals on days 1 and 6 to produce the dashed lines on the graphs (Figures 2D and 2E), or subtracted from individual partner time to produce Figures S1B and S1C.

Focal voles were anesthetized with isoflurane and implanted with a subcutaneous RFID tag (BioMark) between the shoulder blades. Focal voles were then placed into the RFID-tracked habitat in groups of four females of the same genotype ($Oxtr^{+/+}$ or $Oxtr^{1-/-}$). Each trial contained two pairs of two voles (four in total). Each pair of voles lived with their respective partner from weaning, a duration more than sufficient to establish peer partner preference.²⁶ Since RFID tracking only acquires data for animal position (and lacks behavioral details), we conducted and recorded 10-minute social interaction tests with all four animals before and after the week of group housing in the RFID habitat (Figure S1A).

Social operant conditioning

Training and social testing were conducted according to a previously described operant social choice protocol.⁴⁰ Each training apparatus (30.5 cm × 24.1 cm × 21.0 cm) was equipped with a lever, a clicker, and a treat dispenser which released a 20 mg food pellet upon lever press or manual reinforcement. Voles were initially trained to lever press via manual reinforcement in response to lever investigation. Once the vole learned to press independently, it was moved to the second phase of food training at fixed ratio 1. After 3 sequential days of fixed ratio 1, the voles were moved to fixed ratio 4 for 5 days. A subset of animals that met the previously described training criterion²⁰ were designated as focal animals and proceeded to social testing. The training criterion is defined as 3 consecutive days of ≥ 5 responses with no manual reinforcement within the first 2 weeks of training.

Social testing took place in a modular testing apparatus with three chambers (15 cm × 20.5 cm × 13 cm). The center chamber was equipped with two motorized doors and two levers, one of each on either side. A clear plastic tube connects both outside chambers to the center chamber. Prior to social testing, each vole was habituated to the social testing apparatus for 3 days during which the voles learned that each lever opened a door to the corresponding side chamber with a social stimulus rather than a food reward. Before each test, the focal animal was placed into the center chamber where it could press either lever to open the corresponding door allowing access to the reward within the respective chamber for one minute. After one minute the door closes the experimenter moves the focal animal back to the center chamber. Each trial lasted 30 minutes and was recorded for behavioral scoring by a trained observer who was blind to the subject’s experimental group.

Social choice testing occurred in four phases: (1) peer partner versus peer stranger, (2) mate partner versus mate stranger, (3) mate partner versus novel object. Each social testing context was repeated for 3 days. The testing order and novel objects remained the same for both treatment groups. All male partners were castrated and implanted with a testosterone capsule 10-15 days prior to pairing with female focal animals.²⁰

Body weight and temperature

Four solo-housed adults (P60-80) of each genotype were weighed and anesthetized using isoflurane. Each vole was subcutaneously injected with ISO FDX-B thermal sensing PIT tags (BioTherm13, Biomark). Body temperature was monitored for one week in

30-second intervals using an RFID antenna base beneath each cage. The data were processed using ClockLab (Actimetrics/Lafayette Instruments) and averaged for comparison across genotype groups.

Near-infrared oxytocin imaging with nanOx nanosensors

Synthesis of ssDNA-SWCNT nanosensors

ssDNA-SWCNT nanosensors were prepared as described previously.⁴⁴ Briefly, HiPCo SWCNT slurry (NanoIntegris) and ssDNA (Integrated DNA Technologies) were mixed in a 1.5 mL DNA LoBind tube to a final volume of 1.2 mL with a final NaCl concentration of 10 mM. The mass ratio of DNA to SWCNT was 2:1. The DNA sequence was CCCCCACGGGACCGCAGATCGAGCCCCC. The mixture was probe-tip sonicated (Cole-Parmer Ultrasonic Processor, 3-mm tip) in ice-cold water for 30 min at 50% amplitude. The resulting suspensions were centrifuged at 21,000 g for 240 min to pellet unsuspended SWCNT. Nanosensor concentration was calculated by measuring absorbance at 632 nm (NanoDrop One, Thermo Scientific) with an extinction coefficient of $\epsilon = 0.036 \text{ (mg/L)}^{-1} \text{ cm}^{-1}$. Nanosensors were diluted to 200 mg/L in 10 mM stored at 4°C.

Acute slice preparation and nanosensor labeling

Acute brain slices were prepared following the protocols described previously.^{44,47} Cutting buffer (119 mM NaCl, 26.2 mM NaHCO₃, 2.5 mM KCl, 1 mM NaH₂PO₄, 3.5 mM MgCl₂, 10 mM glucose) and aCSF (119 mM NaCl, 26.2 mM NaHCO₃, 2.5 mM KCl, 1 mM NaH₂PO₄, 1.3 mM MgCl₂, 10 mM glucose, 2 mM CaCl₂, all purchased from Sigma-Aldrich) were prepared and bubbled with carbogen gas (oxygen/carbon dioxide 95% O₂, 5% CO₂, Praxair). The animals were deeply anesthetized via intraperitoneal injection of ketamine (120 mg/kg) and xylazine (24 mg/kg) and transcardially perfused with 5 mL of ice-cold cutting buffer. The brain was subsequently extracted, mounted on a vibratome cutting stage (Leica VT 1000) in the carbogen-bubbled cutting buffer, and cut into 300 μm thick coronal slices with microtome razor blades (Personna, double edge super blades; VWR). Slices were incubated at 37°C for 30 min in oxygen-saturated aCSF in a chamber (Scientific Systems Design, Inc., BSK4) and then transferred to room temperature for 30 min. To label the slice with nanosensors, slices were transferred to a separate incubation chamber (Scientific Systems Design, Inc., BSK2) filled with 5 mL of carbogen-bubbled aCSF at room temperature. Nanosensors were applied to the surface of brain slices with a pipette to a final concentration of 2 mg/L and incubated for 15 min. Slices were rinsed for 5 sec with bubbled aCSF through 3 wells of a 24-well plate to remove unlocalized nanosensors, transferred back to the main chamber, and rested for at least 15 min before imaging.

nIR microscope design

A custom upright epifluorescence microscope (Olympus, Sutter Instruments) described in greater detail previously^{44,47} was used to image nanOX and NIRCAt fluorescence responses for nanosensors embedded in the extracellular space of acute brain slices. Briefly, a 785 nm excitation laser (OptoEngine LLC, MDL-III-785R-300mW) was used to excite nanosensors, and nanosensor fluorescence was collected with a two-dimensional InGaAs array detector (Raptor Photonics, Ninox 640). Microscope operation was controlled by Micro-Manager Open Source Microscopy Software 42.

Electrical stimulation evoked neurochemical imaging with nIR microscope

Carbogen-bubbled aCSF was flown through the microscope chamber with a perfusion pump (World Precision Instruments, Peri-Star Pro) and an aspirator pump (Warner Instruments, Dedicated Workstation Vacuum System) at a rate of 2 mL/min. Imaging chamber temperature was kept at 32°C with an inline heater with feedback control (Warner Instruments, TV-324C). Slices labeled with nanosensors were placed in the chamber with a Tissue harp (Warner Instruments), and a bipolar stimulation electrode (MicroProbes for Life Science, PI2ST30.1A5) was positioned to the targeted field of view, which was adjusted with a 4X objective (Olympus XLFluor 4X/340). Next, NIR imaging was accomplished with a 60X objective (Nikon, CFI Achromat NIR 60X W) and the imaging field of view was positioned at least 80 μm away from the stimulation electrode. Using Micro-Manager, nIR fluorescence images were acquired at frame rates of 8 frames/s (nominal) for 600 frames, where 1 millisecond of 0.5 mA stimulation was applied at after 200 frames of baseline. This image acquisition was repeated three times with the same field of view, with 5 min of waiting time in between. Note that the electrical stimulation of neurons does not provide cell specificity, potentially leading to the release of other neurochemicals near the electrodes, and nanOx shows response to dopamine while exhibiting selectivity towards other molecules.⁴⁴ Therefore, to achieve oxytocin selectivity, 2 μM of quinpirole (Fisher Scientific, 10-611-0), a D₂ receptor agonist known to suppress dopamine release,⁴⁷ was applied to the chamber through aCSF perfusion and slices were incubated for 15 min before imaging (see Figures S4A–S4E for the dataset without quinpirole application). Images were acquired in the same field of view before quinpirole application (three replicates) with 5 min between each replicate stimulation.

Image processing and data analysis of nanosensor fluorescence response

Imaging movie files were processed using a custom Python code (<https://github.com/NicholasOuassil/NanoImgPro>) (schematically summarized in Figures S3B–S3D). Integrated $\Delta F/F_0$ ($\Delta F/F_0$ for the entire field of view, 175 μm by 140 μm) (Figures 4D, 4E, and S3B) was calculated as $\Delta F/F_0 = (F - F_0) / F_0$, where F_0 is the average intensity for the first 5% of frames and F is the dynamic fluorescence intensity from the entire field of view and averaged over three stimulation replicates. Next, a 25x25 pixel (corresponding to 6.8 μm by 6.8 μm) grid mask was applied to the image stack (Figure S3C) to minimize bias and improve stack processing time, and then a median filter convolution within each grid was calculated. For each grid square, $\Delta F/F_0$ was calculated, and regions of interest (ROI) were identified if the F at the time of stimulation (200 frames) was 3 standard deviations above the baseline F_0 activity (Figure S3D). Subsequently, the number of ROIs identified from three stimulation replicates was averaged and called the number of release sites. Lastly, $\Delta F/F_0$ was averaged over all identified ROIs, corresponding to the $\Delta F/F_0$ across active release sites (Figure S3E). $\Delta F/F_0$ for the entire field of view can also be obtained by applying a 640x640 pixel to the Python code above. The

grid size dependence and the threshold value dependence of each parameter were evaluated to identify optimal values for each parameter (Figures S3F–S3I).

QUANTIFICATION AND STATISTICAL ANALYSIS

All data are shown as means±standard error of the mean (SEM). Statistical significance is determined by an α of 0.05. Analysis of Variance (ANOVA) was used for comparing multiple groups and general linear mixed models (GLMM) were utilized for experiments in which subjects underwent repeated days of testing. Significant effects were followed up with post hoc comparisons using t-tests, including paired, unpaired (Student's or Welch's, depending on variance equality), or one-sample t-tests, as appropriate for the data structure and experimental design. All statistical tests, effects, and sample sizes for primary and supplementary figures are articulated in the supplementary data tables or figure captions, respectively. GraphPad Prism 10 or JMP Pro 17 were used for all data analysis. All data were included in analyses and figures unless they met predefined exclusion criteria, which included incomplete behavioral testing, lost or corrupted video recordings, or mis-sexing of stimulus animals.